**Development of Angiotensin II Receptor Blocker Nanoparticles for an Inhaled Therapeutic Treatment of COPD via TGF-Beta Antagonism**

by

Michael G. Sweet

A thesis submitted to Johns Hopkins University in conformity with the requirements for the degree of Master of Science in Engineering

Baltimore, Maryland
May 2019

## Abstract

Chronic obstructive pulmonary disease (COPD) is a widespread, progressive lung disease that is characterized by airspace enlargement, inflammation, sputum production, and airway remodeling. Current treatments target and manage symptoms while failing to treat the underlying cause of COPD. Previous studies have shown that overexpression of transforming growth factor beta (TGF-β) is a primary factor in the pathogenesis of COPD. We have previously shown that angiotensin II receptor blockers (ARBs) can antagonize TGF-β expression via angiotensin II type 1 receptor blockage. We have successfully developed a localized treatment for cigarette-smoke induced lung injury through TGF-β antagonization using the ARB Telmisartan (TEL). Here, I have begun the investigation into four ARBs, formulated as nanocrystals, for inhaled localized treatment of COPD. We hypothesized that by using F127, a surfactant known as pluronic polymer we can develop muco-inert nanocrystals with increased retention time, improved pharmacokinetics, and therapeutic efficacy while reducing administration concentrations. Four ARBs were formulated as nanocrystal with three pluronic polymers. Surface characterization was controlled via choice of pluronic polymer. I found that pluronic polymer F127 provided ideal surface stabilization and improved retention time through assumed mucus penetration and macrophage uptake resistance. ARB nanocrystals {ARB-NC's) were shown to have a favorable linear release profile *in vitro* as well as drug activity unaffected by the coating. *In vivo* investigation suggest F127/ARBs may have improved pharmacokinetics, but additional research is required to confirm. Finally, an accurate COPD murine model was used to test for TGF-β expression antagonism and therapeutic effect of inhaled F127/TEL nanocrystals both of which showed positive effect. Thus, I conclude that F127/ARB nanocrystals

can provide a therapeutic treatment for COPD and further investigation should continue with the ARBs used in this study and others currently on the market.

Advisor: Dr. Jung Soo Suk

Reader: Dr. Laura Ensign-Hodges

**Acknowledgements**

First, I would like to acknowledge my parents for affording me the opportunity to return home and pursue my master's degree at Johns Hopkins with their full support and unconditional love. I would like to thank the rest of my family, Billy, Brigit, Jack, Roman, Moe, and Bayly, for helping me to keep my head afloat in these difficult two years as well as those previous.

I would like to thank my research advisor Dr. Jung Soo Suk for giving me a position on his team and the opportunity to conduct research in this incredible lab. I would like to thank Dr. Laura Ensign-Hodges for taking the time to be my thesis reader.

I would especially like to thank my mentor Dr. Daiqin Chen. While sometimes it seems as though it is forgotten that master's students are still just students, you provided me a space to learn and grow as a person and researcher and I am forever grateful for that. Thank you to Jinhao Liu, as well, for being a valuable member of our team as well as a friend. I wish the both of you the best of luck both at Hopkins and in your future endeavors.

I also need to thank the other members of the Center for Nanomedicine for making it such a wonderful place to work. No matter how difficult the days could get, the members of the CNM made it worth showing up to work. It has truly been a privilege to work among this talented group of researchers.

Finally, thank you to all my friends for always being around even when I wasn't. An important factor in keeping my spirits up has always been knowing my friends were close if I ever needed to talk or blow off some steam.

**Table of Contents**

## List of Tables

## List of Figures

## 1. Introduction and Background

### 1.1 Chronic Obstructive Pulmonary Disease

Chronic Obstructive Pulmonary Disease (COPD) is a progressive lung disease defined by restricted airflow from the lungs, inflammation, airway remodeling, and emphysema [1]. COPD is the 3rd leading cause of death in the United States and 10th globally which resulted in ~3.2 million deaths in 2015 [2]. Although genetics and environmental pollutants play a role in COPD risk, the main cause for COPD is cigarette smoke inhalation [2]. Unfortunately, the effects of COPD are largely irreversible; however, common treatments such as $\beta_2$-agonists and anticholinergic agents paired with corticosteroids can provide symptomatic relief [3]. As COPD cases continue to rise worldwide [2], a therapeutic treatment that can target and halt the progression of COPD is increasingly imperative.

### 1.2 TGF-β

Transforming growth factor (TGF) is a superfamily of regulatory proteins with a wide variety of functions throughout the body. TGF-β is a subfamily consisting of the TGF-β1, TGF-β2, and TGF-β3 isoforms that play an important role in the development and maintenance of the lungs [4]. Dysregulation of TGF-β signaling, leading to increased TGF-β, has been observed in patients with COPD and other lung diseases [4,5]. Additionally, cigarette smoke has been shown to increase TGF-β signaling which leads to inflammation of the airways, cell death, and airway remodeling [5-7]. Most importantly, antagonization of TGF-β signaling has been proven to reduce airway remodeling [7,8]. Reducing or eliminating TGF-β dysregulation is an appealing option for the development of a therapeutic treatment for COPD.

### 1.3 Limiting TGF-β Expression Via AT1R Antagonization

Angiotensin II receptor blockers (ARBs) are a widely used anti-hypertension medications that work by blocking the angiotensin II type 1 receptor (AT1R). Angiotensin II has been linked to increased production of TGF-β as well as the activation of latent TGF-β [9]. Additionally, Angiotensin II has been shown to play an important role in increased alveolar epithelial cell apoptosis via the AT1R pathway [10]. AT1Rs have been detected within alveolar Type I cells which comprise around 95% of the alveolar surface [11]. Angiotensin II's connection to TGF-β expression, combined with the abundance of AT1R present in the lung, make ARBs an ideal candidate for a localized treatment of COPD.

### 1.4 Losartan as a Preventative Treatment for Cigarette Smoke Induced Lung Injury

The first step within our group's study was to prove ARBs could prevent lung damage through TGF-β antagonization [12]. The study investigated the effects of the ARB Losartan on a murine model of chronic cigarette smoke (CS) induced lung injury. It was demonstrated that daily oral doses of Losartan effectively inhibited TGF-β signaling. The decrease of TGF-β signaling lead to alleviated oxidative stress, inflammation, metalloprotease activation, and elastin remodeling. Although effective, this treatment model can only serve as a preventative treatment for COPD. Additionally, the high dosing concentration of 30mg/kg would likely cause severe side effects. Despite the flaws, the study did prove that ARBs can provide effective treatment of lung injury via TGF-β antagonism.

### 1.5 Overcoming the Mucus Membrane Via Polymer Coating

In order to improve the specificity and effectiveness of ARBs for the treatment of COPD, it was proposed that an inhaled particle may overcome the shortcomings of the initial treatment model. A localized inhaled treatment, however, does introduce new challenges, including the mucus barrier. Mucus is a viscoelastic, porous, adhesive gel that lines the epithelium and removes particulates through mucociliary clearance (MCC) [13,14]. Any particle which adheres to the mucus barrier would have a greatly reduced therapeutic window. It was proven that high densities of low molecular weight polyethylene glycol (PEG) could effectively make polystyrene nanoparticles muco-inert [15] and that prior findings that PEGylated particles were mucoadhesive were misattributed to the PEG coating [16]. We have previously demonstrated the successful mucosal penetration of pluronic polymer F127 coated nanoparticles using the fluorescent drug Curcumin [17]. The formulation of the Curcumin nanosuspension provides the basis for the development of the ARB nanocrystals. As ARBs are not easily trackable, it is assumed that the mucus penetrating properties of the Curcumin nanoparticles provided by the pluronic polymer coating will transfer to the pluronic polymer ARBs.

### 1.6 Telmisartan Nanocrystals as a Treatment of Lung Injury and Emphysema

In an unpublished recent study by our group, a nanosuspension (NS) of Telmisartan (TEL), a type of ARB, was developed based on the curcumin mucus penetrating particle (MPP) formulation. Importantly, the particles had similar size and charge to those of the curcumin particle [Table 1]. The F127 coated particles showed favorable *in vitro* particle stability, macrophage uptake resistance, and drug activity. Pharmacokinetic data showed improved drug

retention compared to free drug (FD) alternatives. For *in vivo* experimentation, mice either received daily oral doses of free drug or bi-weekly intratracheal doses of TEL-NS at 1mg/kg. Concurrent treatment of an acute cigarette smoke induced lung injury murine model showed decreased TGF- β expression similar to the initial Losartan experiment, denoting effective protection from injury. Therapeutic effect was tested using a TSK transgenic murine model of emphysema [18] . The treatment of the transgenic mice also showed decreased TGF- β expression as well as partial reversal of airway enlargement while free drug had no effect. This study provided the first evidence of the therapeutic effect of ARBs for lung injury. In order to improve on this research, three factors were considered: (1) development of a particle in powder form, (2) investigation of additional ARBs, and (3) testing on a more accurate murine model of COPD.

## 2. ARB Nanoparticle Formulation and Characterization

### 2.1 Introduction

Previous studies have shown the effectiveness of pluronic polymer coating to increase solubility, bioavailability, and improve mucosal penetration [Tao]. Pluronic polymers are triblock copolymers comprised of a hydrophobic polypropylene oxide (PPO) core and hydrophilic polyethylene glycol (PEG) tails, each in varying lengths. Furthermore, this technology has been applied to the ARB Telmisartan effectively. However, Telmisartan is only one of nine ARBs currently available on the market, all of which vary in ways such as potency, bioavailability, and pharmacokinetics [19]. Additionally, the initial TEL formulation was developed as a nanosuspension which was prepared as needed, an impractical element for

widespread use. I sought to develop a NC formulation for four ARBs that could be preserved in powder form and maintain the characteristics of the initial NS formulation.

## 2.2 Methods

### 2.2.1 Formulation of ARB-NC

TEL, IRB, AZL and pluronic polymers were combined in a mass ratio of 1:4, with typical batches of 3mg:12mg, and dissolved in 2mL of chloroform. CAN differs as it was mixed in a ratio of 1:2, with typical batches of 3mg:6mg, and dissolved in 2mL of methanol. Once completely dissolved, the solvent was evaporated with nitrogen gas. In order to ensure complete solvent evaporation, the samples were vacuum dried overnight. Samples were resuspended in ultrapure water to 0.1w/w% (only considering ARB mass) and placed in a sonic bath for 15min. The samples were then sonic probed (Sonics VCX-500 ultrasonic processor) for 1hr with a 1s on/off cycle (30min on, 30min off total) and 40% amplitude. The sample was then centrifuged for 10min at 3000 rpm to remove large particles. The supernatant was collected and run through centrifugal filter (Amicon Ultra 30K) at 17,000g. The collected crystals were then washed in triplicate by thoroughly resuspending in 0.05% Tween 80 ultrapure water and re-filtered in the centrifuge for 10min at 17,000g. Finally, the nanocrystals were resuspended in ultrapure water and removed to a vial. For storage, 6w/w% trehalose dihydrate was added as a cryoprotectant and the sample was frozen using liquid nitrogen and vacuum dried overnight.

### 2.2.2 Characterization of ARB-NC

The ARB-NC's were resuspended in ultrapure water and diluted 10x in 10mM NaCL at pH 7. The particle size and ζ-potential were measured using the Dynamic Light Scattering and

Laser Doppler Anemometry functions of the Malvern Zetasizer Nano. Measurements were performed at 25ºC with a scattering angle of 90º. A Hitachi H7600 Transmission Electron Microscope (TEM) was used to image the particles. The ARB-NC's were rehydrated at 0.1w/w% (only considering ARB mass) and 10µL was added to a copper TEM disk grid and allowed to dry overnight.

**2.3 Results and Discussion**

The ARB-NC synthesis method was derived from the Curcumin-MPP method as previously mentioned. This preparation technique is relatively quick, simple, and easily repeatable; it lacks the need for expensive/unique equipment which makes it an appealing preparation technique. The synthesis technique relies on the hydrophobic interactions between the drugs and the hydrophobic polypropylene oxide core of the pluronic polymer. I have chosen the four ARBs for this study based on their logP value [Table 2], an indicator of hydrophobicity, as a gauge of their ability to form nanocrystals. Losartan was discarded despite previous success as its active metabolite, EXP3174, is formed in the liver [19]. Compared to the Curcumin formulation, the hydrodynamic diameter of the ARB-NC [Table 1] is much larger at ~280nm for F127/TEL, F127/AZL and ~260nm for F127/IRB, F127/CAN but still fall within the expected viable size range around 300nm [17,20]. The particles tend to increase in size from F127 to F98 to F68 coating indicating that F127 is the strongest surface stabilizer. Additionally, the ζ-potential increases in magnitude from a desirable near 0 ζ -potential for F127 coatings to ζ -potential in the mid to high teens for F68 coatings. The near 0 ζ-potential of F127 coated particles indicate a stable, uniform coating while the increased charges of the F68 coated particles indicate a non-uniform or incomplete particle coating [21]. F127 and F98 coated particles also show low Poly

Dispersity Index (PDI) values indicating batch uniformity. The characteristics between F127 and F98 are generally very similar with F127 consistently having a slightly smaller ζ-potential and size. Due to the similarity of these two particles, F127 was chosen as the primary candidate for continued research due to its slightly favorable characteristics. TEM images of the F127/ARB particles show rod shaped particles for F127/TEL, F127/IRB, and F127/CAN and an irregular structure for F127/AZL [Figure 1].

**Table 1.** Size, uniformity, and charge characteristics of 12 ARB-NC formulations.

| ARB | Formulation | Z-Average (nm)[a] | PDI | ζ-potential (mV) |
|---|---|---|---|---|
| Curcumin (CUR)[b] | F127/CUR | 133 ± 12 | - | -0.80 ± 0.1 |
| Telmisartan (TEL) | F127/TEL-NS | 110 ± 7 | 0.2 | -2 ± 0.2 |
| Telmisartan (TEL) | F127/TEL | 278 ± 3 | 0.186 ± 0.04 | -1.74 ± 0.6 |
| | F98/TEL | 306 ± 6 | 0.236 ± 0.06 | -4.01 ± 2.5 |
| | F68/TEL | 334 ± 12 | 0.366 ± 0.14 | -18.36 ± 2.1 |
| Azilsartan (AZL) | F127/AZL | 280 ± 5 | 0.243 ± 0.08 | -2.71 ± 0.8 |
| | F98/AZL | 320 ± 7 | 0.204 ± 0.01 | -3.81 ± 0.9 |
| | F68/AZL | 345 ± 9 | 0.394 ± 0.02 | -13.13 ± 1.6 |
| Irbesartan (IRB) | F127/IRB | 260 ± 3 | 0.145 ± 0.03 | -2.21 ± 0.4 |
| | F98/IRB | 244 ± 9 | 0.139 ± 0.01 | -4.19 ± 1.3 |
| | F68/IRB | 292 ± 4 | 0.170 ± 0.02 | -12.4 ± 1.5 |
| Candesartan (CAN) | F127/CAN | 263 ± 4 | 0.172 ± 0.03 | -4.30 ± 0.4 |
| | F98/CAN | 284 ± 4 | 0.219 ± 0.04 | -5.72 ± 2.2 |
| | F68/CAN | 292 ± 10 | 0.349 ± 0.11 | -15.01 ± 1.0 |

[a] Z-Average is a measurement of hydrodynamic size

[b] [17]

**Table 2.** ARB candidates for NC formulation and their respective logP values.

| ARB | logP |
|---|---|
| Telmisartan (TEL) | 6.04 |
| Azilsartan (AZL) | 5.70 |
| Irbesartan (IRB) | 5.50 |
| Candesartan (CAN) | 5.17 |
| Losartan (LOS) | 5.06 |

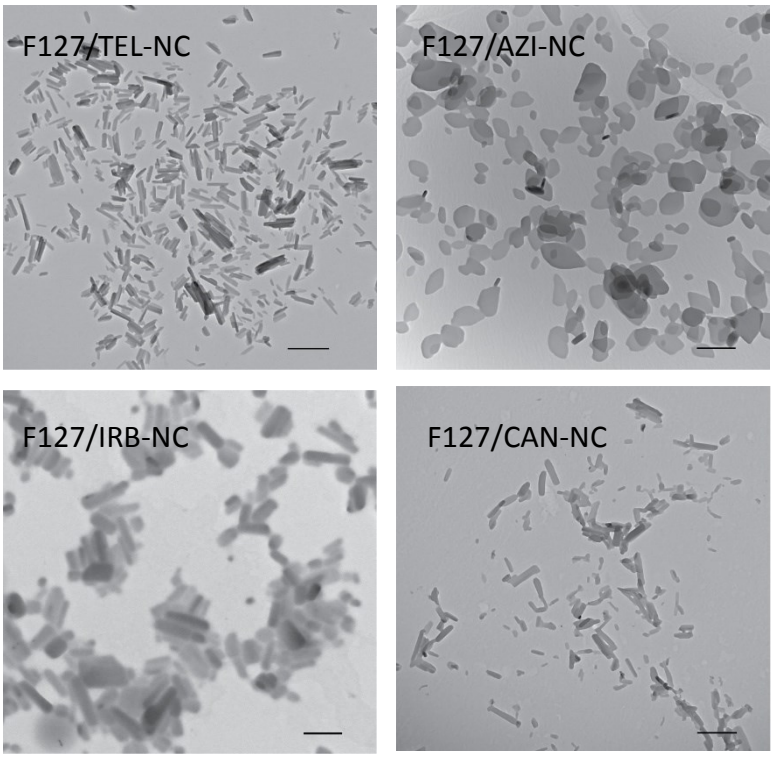


**Figure 1.** Transmission Electron Microscopic (TEM) images of F127/ARB formulations.

# 3 *In Vitro* Studies

## 3.1 Introduction

After confirming the ARB-NCs fit the parameters of the Curcumin-MPP model, the next step was to test *in vitro* characteristics. Four parameters were tested in the *in vitro* stage: (1) stability in biological conditions; (2) resistance to macrophage uptake; (3) drug release profile; and (4) drug activity. In order to retain the mucus penetrating properties of the muco-inert coating, the ARB-NC must resist aggregation in biological conditions to avoid steric entrapment and clearance. The ARB-NC should also show improved resistance to macrophage uptake and clearance. The development of a drug release profile will determine if the particle coating serves as a quick or slow release drug, either of which could be a favorable trait in future studies. Finally, and perhaps most importantly, the ARB-NC need to maintain their intrinsic drug properties otherwise they serve no purpose.

## 3.2 Methods

### 3.2.1 ARB-NC Stability in BALF

ARB-NC stability was tested in BALF (Bronchial alveolar lavage fluid). BALF was collected from C57 BL/6 male mouse lungs by lavage with 1mL Dulbecco's Phosphate Buffer Solution (DPBS) repeated three times. BALF was centrifuged at 1500g to remove cells and the supernatant was collected. BALF protein concentration was measured using a Pierce BCA protein assay kit (ThermoFisher Scientific). A standard was created via serial dilution of given BSA ampules with DPBS. 200µL of working reagent was added to 25µL of each sample and the microplate was incubated and shaken at 37ºC for 30min. Absorbance was measured at 562nm

(BioTek Synergy Mx Microplate Reader) and sample concentrations were plotted against the standard curve. BALF was diluted to a concentration of 0.6mg/mL with DPBS. ARB-NC were resuspended in ultrapure water and diluted to a concentration of 10mg/mL. 40µL of ARB-NC was added to 400µL of BALF and incubated at 37ºC. Hydrodynamic size measurements were measured at 0, 2, and 6hrs using DLS (Malvern Zetasizer Nano).

### 3.2.2 Alveolar Macrophage Uptake Resistance

Mouse alveolar macrophage cells (MH-S) were maintained in accordance with ATCC guidelines. For the experiment the cells were subcultured into sic well plates for two days to achieve confluence ≥ 85%. 100µM concentrations of F127/ARB and F68/ARB in cell culture media were prepared. Standard media was withdrawn from each well and the cells were washed with DPBS. 1mL of 100mM NC media was added to each well and was incubated for two hours. After the incubation period, the cells were detached and collected using Trypsin. The collected cells were washed in triplicate by suspending in 1mL of DPBS, centrifuging at 12000rpm for 1min and disposing of the supernatant. After washing, the cells were resuspended in 0.5mL of DPBS and probe sonicated (Sonics VCX-500 ultrasonic processor) for 5min with a 5/10s on/off cycle (1:40min on, 3:20min off total) and 40% amplitude. A Pierce BCA protein testing kit (ThermoFisher Scientific) was used to determine cell concentration as described before. The remaining sample was diluted 2x with methanol, centrifuged at 12000rpm for 1min, and the supernatant was collected. A standard was created via serial dilution of a freshly prepared 1mg/mL stock solution of ARB-FD in DMSO with a stock methanol: DPBS solution. Standard and samples were analyzed using HPLC (Shimadzu Prominence-I Series HPLC with RF-20a) fluorescence detector with drug specific settings [Table 3].

**Table 3.** HPLC settings for ARB fluorescence detection.

| **ARB** | Excitation λ (nm)[a] | Emission λ (nm) | Mobile Phase |
|---|---|---|---|
| Telmisartan (TEL) | 300 | 360 | 70% $H_2O$ 0.01%TFA<br>30% MeOH |
| Azilsartan (AZL) | 299 | 368 | 60% $H_2O$ 0.01%TFA<br>40% MeOH |
| Irbesartan (IRB) | 260 | 374 | 60% $H_2O$ 0.01%TFA<br>40% MeOH |
| Candesartan (CAN) | 296 | 371 | 50% $H_2O$ 0.01%TFA<br>10% MeOH<br>40% ACN |

Note. All separations performed using a Phenomenex Luna Omega 5µm Polar C18 100Å 150 x 4.6mm column. Injection volume 25µL. Flowrate of 1mL/min. Ambient temperature.

[a] Excitation wavelength was also used for UV-vis spectroscopy or Photodiode Array (PDA) detection when applicable.

### 3.2.3 Drug Release Profile

The ARB-NC were resuspended in DPBS with 0.05% Tween 80. A standard was created via serial dilution of 1mg/mL ARB-FD in DMSO with stock DMSO: DPBS with 0.05% Tween 80. An aliquot of rehydrated ARB-NC was diluted with an equal measure of DMSO to normalize to the standard. Samples and standards were measured using UV-vis spectroscopy (Fisher Nanodrop 2000) at drug specific wavelengths [Table 3]. The ARB-NC solution was diluted to 4µg/mL with DPBS 0.05% Tween 80. 1mL of ARB-NC solution was added to a dialysis device (Spectrum Spectra-Por Float-A-Lyzer G2 1mL) which was then submerged in 20mL of DPBS 0.05% Tween 80 within a 50mL conical tube. The samples were wrapped in aluminum foil to protect from light and were placed in a plate shake incubator at 37ºC for 5 days. 1mL samples were withdrawn from the 50mL tube at set time points, the tube was refilled with 1mL of fresh

DPBS 0.05% Tween 80 at each point. The samples were analyzed using HPLC (Shimadzu Prominence-I Series HPLC with RF-20a) fluorescence detector as described before.

### 3.2.4 Measurement of Drug Activity

Pulmonary artery smooth muscle cells (PASMCs) were collected and isolated from rats. Heart and lungs were collected and washed with HEPES buffered saline solution (HBS). Intrapulmonary arteries were isolated and digested at 37ºC for 20min in reduced $Ca^{2+}$ HBS with collagenase (type 1, 1750 U/mL), papain (9.5U/mL), BSA (2mg/mL), and dithiothreitol (1mM). Smooth cells were collected, filtered, and cultured in Ham's F-12 media with 0.5% fetal calf serum and 1% penicillin-streptomycin for 24-48hrs. PASMCs were plated at confluence ≥ 50% and loaded with 5μM Fura 2-AM at 37ºC for 1hr before the $Ca^{2+}$ imaging system. Within the system chamber, cells were perfused with modified Krebs solution and bubbled with 16% $O_2$ gas. The system and components were maintained at 37ºC. Cells were perfused for 15min to establish a stable baseline. Intracellular $Ca^{2+}$ was calculated from ratiometric measurements of F340/F380 excitation with $Ca^{2+}$ standard solutions. Cells were treated with 50μL of ARB-NC or ARB-FD 30min prior to treatment with 1μM ANGII. Control were treated with DPBS.

## 3.3 Results and Discussion

The ARB-NC were developed with the important characteristics that were previously discussed. It is important to verify that those characteristics remain the same within the biological system. It is a concern that, after administration of the ARB-NC, there could be

particle aggregation which would increase steric hinderance with the mucus mesh. The stability test that was performed confirmed that F127/ARB-NC are size stable within BALF [Figure 2]. Little to no size change was observed within with first two hours and minimal change from hours two to six. Next it was important to consider if the other biological clearance methods, phagocytes, were capable of nanocrystal clearance. In order to consider the effectiveness of the ARB-NC's resistance to macrophage clearance, F68/ARBs were used as a control. The F68/ARB-NC's were assumed to have poor/uneven pluronic coating based on ζ-potential readings greater than -10mV [Table 1] [21]. Low density PEG coatings were previously proven to be insufficient at preventing hydrophobic interactions between nanocrystals and mucus [16] therefore I assume F68/ARBs act as mucoadhesive particles. The desired outcome was to see a reduced macrophage uptake of F127/ARB crystals compared to the F68/ARBs. For IRB and AZL there are near 2, and 3-fold decreases in uptake while with TEL there is a near 15-fold decrease in macrophage uptake between F127 and F68 coated particles [Figure 3]. Untreated cells were used as a control. Resistance to macrophage uptake will allow the ARB-NC to avoid clearance thereby increasing drug retention. An important factor I considered regarding the therapeutic window was the ARB-NC release profile. The release profile for each ARB-NC tested shows a near linear release over a four-day period [Figure 4]. A linear release profile can help reduce fluctuation of drug levels, as well as decrease dosing frequency, which is important to consider regarding patient compliance [22]. Finally, prior to commencing *in vivo* studies, it was important to prove ARB activity is not inhibited by pluronic coating. To confirm the ARB-NC retained the drugs' intrinsic characteristics, I examined intracellular $Ca^{2+}$ in PASMCs in response to Angiotensin II. Previous studies have shown that ANGII stimulation of AT1R results in increased levels of $Ca^{2+}$ [23]. ARBs are designed to antagonize AT1R and therefore treatment

of cells with ARB-NC should result in decreased $iCa^{2+}$ levels. In each instance, significant reduction in $iCa^{2+}$ can be seen for both ARB-FD and ARB-NC suggesting drug activity has not been inhibited by pluronic coating [Figure 5].

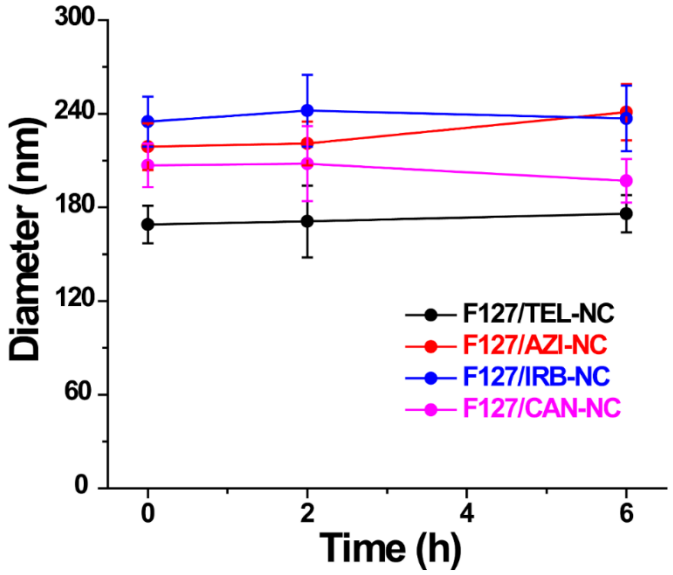


**Figure 2.** Hydrodynamic size, given in number mean (nm), as a function of time showing colloidal stability of F127/ARB-NC in BALF.

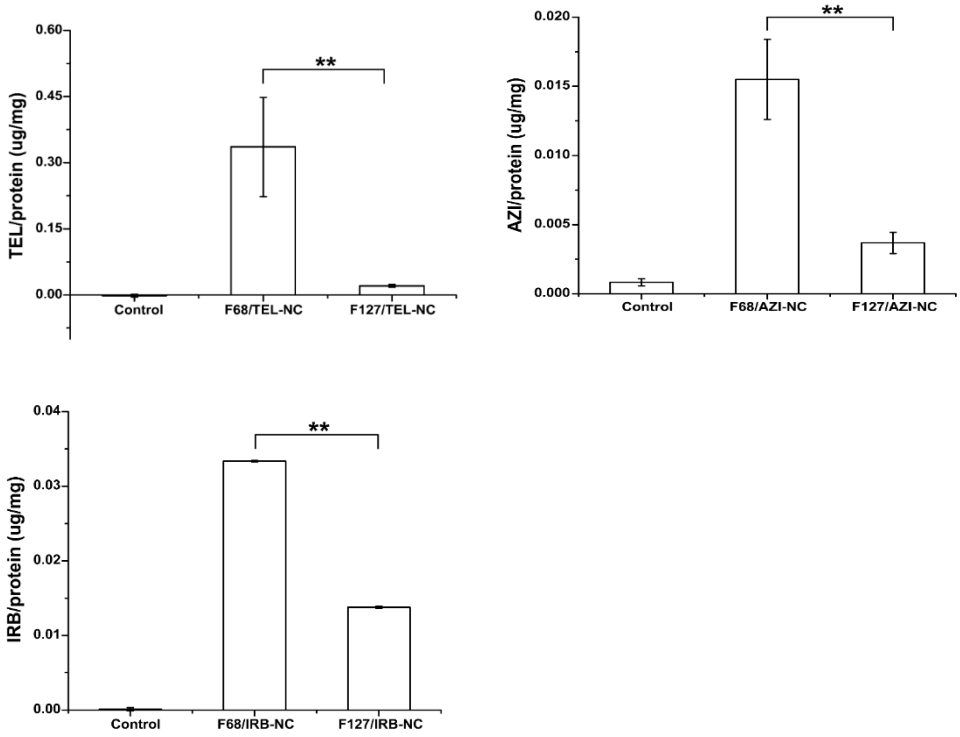


**Figure 3.** Alveolar macrophage uptake of ARB-NC after treatment with 100μM NC-Media Solution and 2hr incubation.

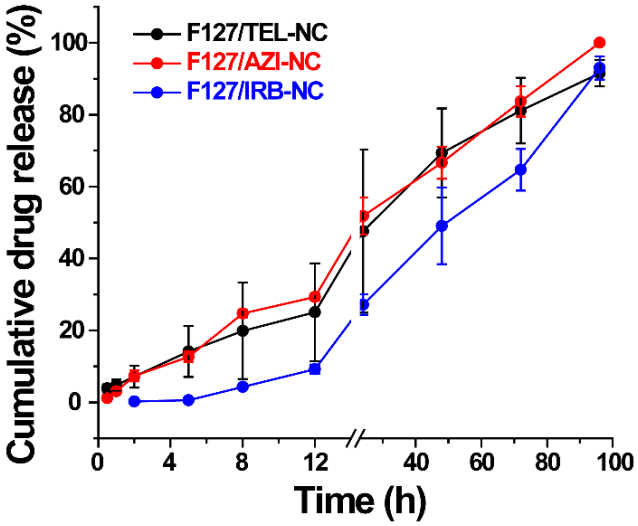


**Figure 4.** Cumulative release of ARB from NC over a four-day period.

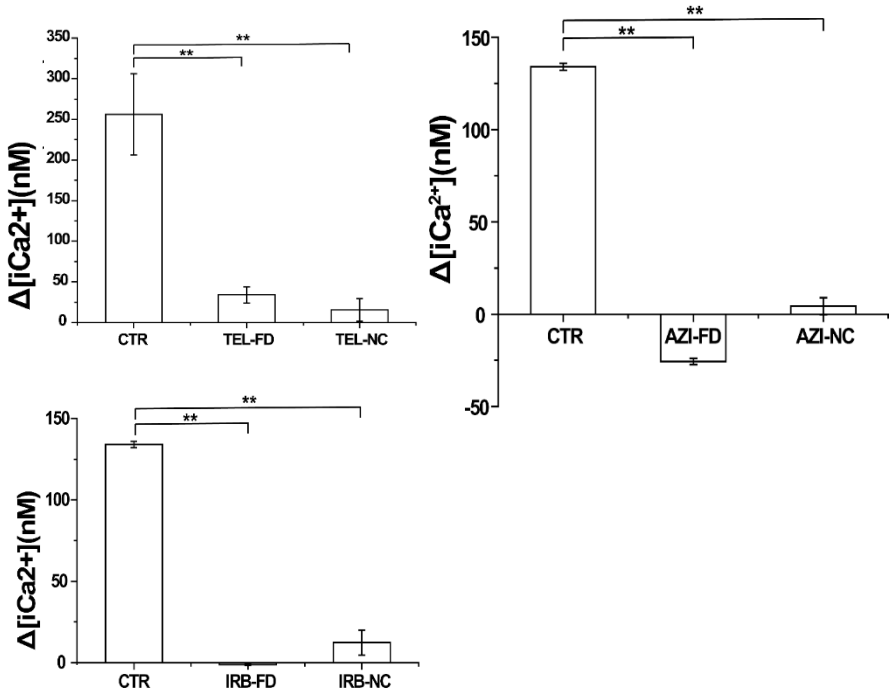


**Figure 5.** Intracellular $Ca^{2+}$ levels measured after exposure to angiotensin II in cells treated with DPBS (CTR), ARB-FD, or F127/ARB-NC.

# 4 *In Vivo* Studies

## 4.1 Introduction

After confirming desirable *in vitro* particle characteristics, three *in vivo* studies were conducted. Due to the extensive time scale of the *in vivo* studies, TEL-NC were chosen as a priority in order to compare the results with our previously conducted study. It is at this stage I can determine drug pharmacokinetics. I hypothesized based on the characteristic and *in vitro* similarity between the ARB-NC and the original TEL-NS that the ARB-NC should show improved 24hr drug retention. For this study, I used a new murine model I believe more

accurately depicts COPD rather than just emphysema. I performed pSmad2 staining to confirm TGF-β inhibition and H&E staining to identify any detectable therapeutic effect of the ARB-NC on airspace structure.

## 4.2 Methods

### 4.2.1 Pharmacokinetics of Two ARB-NC

C57 BL/6 male mice were used to study the pharmacokinetics (PK) of the ARB-NC. Mice were anesthetized with a mixture of Ketamine (17.5%), Xylazine (2.5%), and DPBS (80%) with an injection volume of 5µL/g. The anesthetized mice were intubated according to the *Simple Method of Mouse Lung Intubation* [24] with the additional use of a otoscope as a source of light and magnification. Mice were treated with 0.05mg/kg ARB-NC in aqueous solution. The ARB-NC was driven into the lungs with ~200µL injection of air directly after administration. Five mice were sacrificed at seven varying time points between 0 and 24hrs and the lungs and blood samples were collected. Plasma was separated from blood cells with EDTA treated tubes (Becton Dickinson BD Lavender Tubes) and centrifugation at 4000rpm for 10min. Tissue and plasma samples were dried via lyophilization. Lung samples were crushed with mortar and pestle. Samples were suspended in 0.5mL methanol and homogenized (Qiagen TissueLyser LT) for 10min at 50oscillations per second with ~20 ceramic milling beads per tube. Samples were centrifuged for 10min at 13300 rpm. Supernatant was collected and filtered with 0.45micron PTFE syringe filter (ThermoFisher). Samples were analyzed using HPLC as described before.

### 4.2.2 pSmad2 Staining of F127/TEL Treated CC10-IL-13 Transgenic Mice

CC10-IL-13 Transgenic mice were used for pSmad2 staining. COPD was induced in the transgenic mice via treatment with 0.5% doxycycline water for two months. The mice were then administered 0.05mg/kg doses of ARB-NC or FD every other day for one month. The mice were sacrificed, and the lungs were inflated with agarose and fixed with 4% PFA. Overnight equilibration in cold 4% PFA before sectioning and embedding the lungs in paraffin wax. The sections were deparaffinized and rehydrated in an ethanol series. Antigens were retrieved via incubation in boiling citrate buffer for 10min. The sections were treated with 3% normal serum from chicken and left to remain at room temperature with primary antibodies for 1hr after which the sections were cold incubated at 4ºC for 24hrs. Slides were finally washed with PBS with Tween 20. The pSmad 2/3 antibody was diluted 100x and the staining was developed with the anti-rabbit Ultra Vision detection kit.

### 4.2.3 H&E Staining of F127/TEL Treated CC10-IL-13 Transgenic Mice

CC10-IL-13 transgenic mice were also used for H&E staining. COPD was induced and mice were treated as described before. Lungs were collected and treated as described before. H&E lung section preparation stopped after paraffinization and were stained with H&E.

## 4.3 Results and Discussion

With the continuance of this study, it will be important to improve on the pharmacokinetic data obtained for the ARB-NC. For now, without a FD comparison, conclusive evidence that the ARB-NC provided improved pharmacokinetics is impossible. However, there

is some anecdotal evidence that suggests improved pharmacokinetics. While no definitive conclusions can be drawn, there is a steady decrease in ARB concentration rather than a rapid one, suggesting prolonged retention [Figure 6]. An important component of my *in vivo* data is the use of CC10-IL-13 Tg mice which has been shown to closely resemble COPD [25,26] while the TSK model used before resembles emphysema, a single component of COPD. The stains provide only observational evidence as they have not been quantified. However, from the images pSmad2 expression appears limited in both TEL-FD and TEL-NC as the images most closely resemble the wild type stains rather than the COPD induced transgenic mouse stains [Figure 7]. pSmad2 is a phosphorylated form of the Smad2 protein which becomes phosphorylated as part of the TGF-β signaling pathway [27]. Reduced pSmad2 is a direct result of TGF-β antagonization. The H&E stains appear to show improved alveolar structure in the TEL-NC treated mice, but the extent of repair is unknown [**Figure 8].**

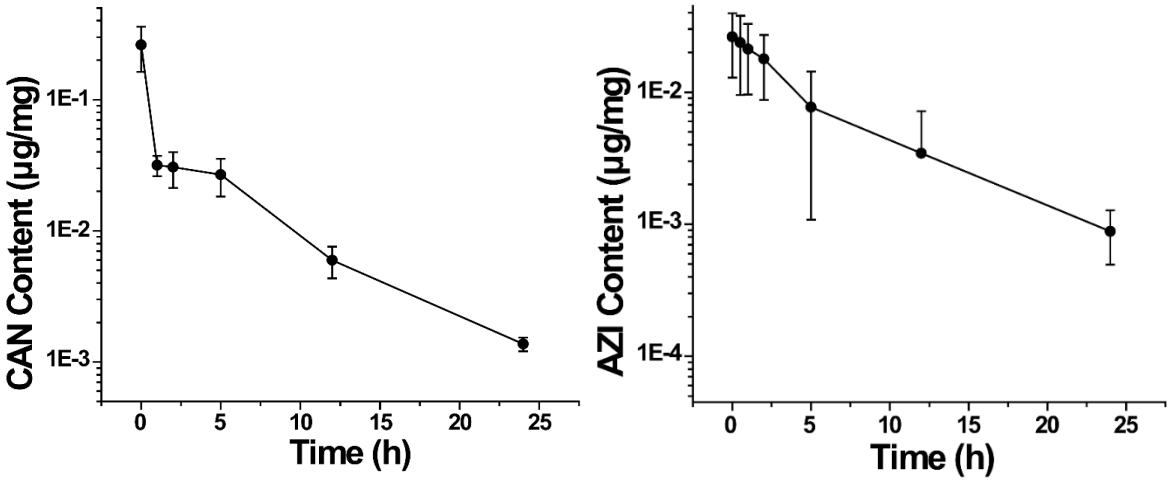


**Figure 6.** ARB concentration measured in the lung of B57 BL/6 male mice as a function of time after intratracheal administration of 0.05mg/kg F127/ARB-NC.

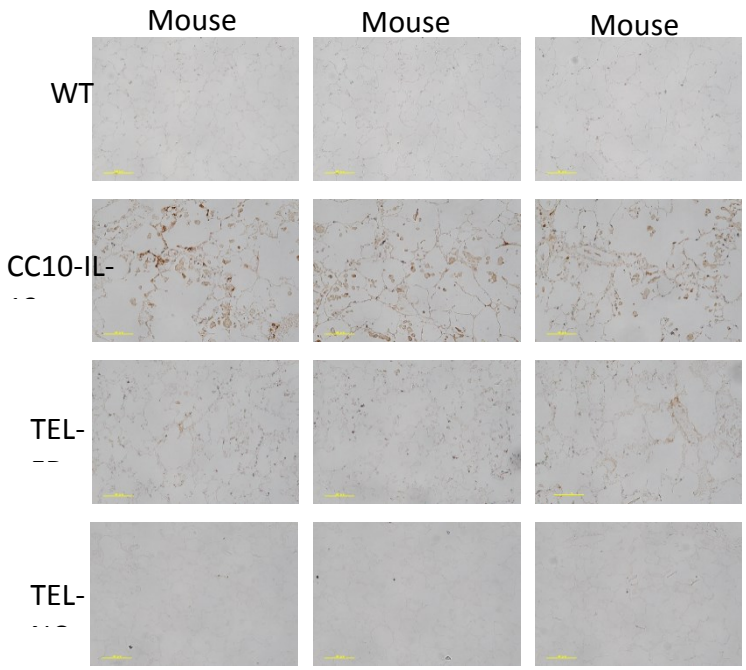


**Figure 7.** Selective staining of the phosphorylated Smad2 (pSmad2) protein in wild type (WT), COPD model (CC10-IL-13), TEL-FD and TEL-NC treated COPD model mice.

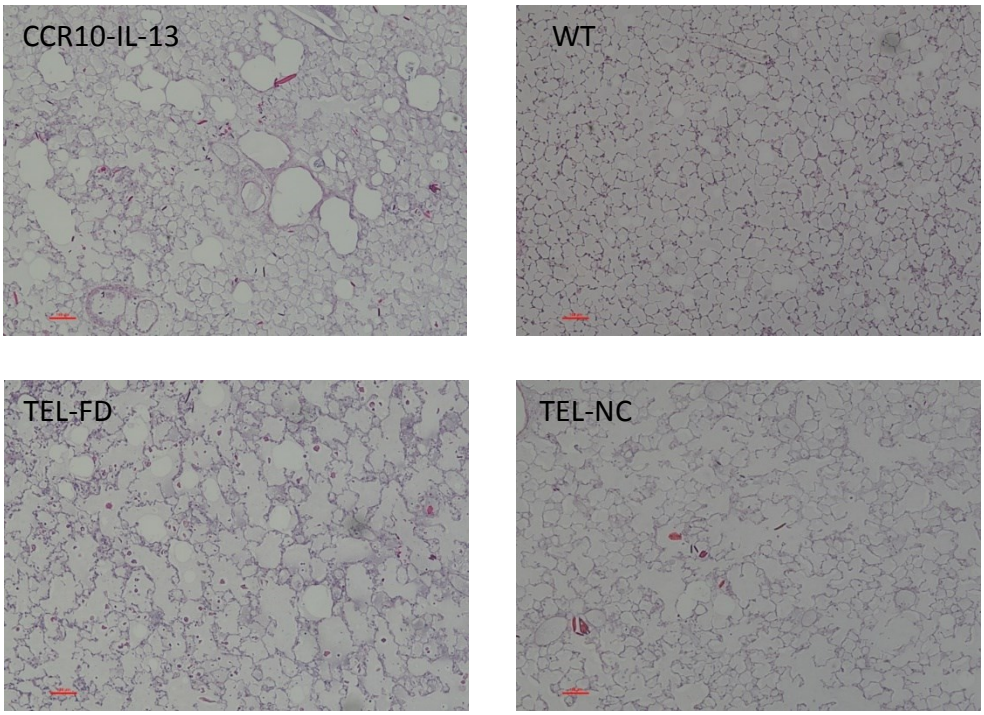


**Figure 8.** H&E staining of wild type (WT), COPD model (CC10-IL-13), TEL-FD and TEL-NC treated COPD model mice. Enlarged airspace can be seen in the COPD model mice.

# 5 Conclusion

In this study, I began the investigation into four ARBs in nanocrystal formulations for the localized therapeutic treatment of COPD. All four ARBs were successfully formulated for powder state storage with size, ζ-potential, and stability indicative of an MPP. The findings show F127 coated ARBs are resistant to macrophage clearance. Additionally, the linear release profile of the ARB-NC suggests infrequent dosing regimes may be achieved. Importantly, I have shown that drug activity is unaffected by pluronic coating. Finally, I have shown through pSmad2 and H&E staining that F127/TEL-NC can inhibit TGF-β expression and act therapeutically on an accurate COPD murine model. It is important to note that this study was part of an ongoing investigation that will continue to work on these ARBs in addition to the other available ARBs. Free drug pharmacokinetic data and quantitative analysis of the staining results will help us optimize dosing regimens and define the effectiveness of ARB-NC as a therapeutic treatment for COPD.

## References


**[1]** Verhamme, F.M, et al., *Transforming Growth Factor-β Superfamily in Obstructive Lung Diseases.* Am J Respir Cell Mol Biol. 2015 Jun;52(6):653-62

**[2]** GBD 2015 Mortality and Causes of Death Collaborators (2016). *Global, regional, and national life expectancy, all-cause mortality, and cause-specific mortality for 249 causes of death, 1980-2015: a systematic analysis for the Global Burden of Disease Study 2015*. Lancet (London, England), *388*(10053), 1459–154 4.

**[3]** Decramer, M, et al. *Chronic Obstructive Pulmonary Disease.* Lancet (London, England), 379(9823), 1341-1351

**[4]** Bartram, U; Speer, C, *The Role of Transforming Growth Factor β in Lung Development and Disease.* Chest. 2004 Feb; 125(2), 754-765

**[5]** Jeffery, Peter, *Remodeling in Asthma and Chronic Obstructive Lung Disease*. Am J Respir Crit Care Med. 2001 Nov; 164(2),

**[6]** Takizawa, H et al. *Increased Expression of Transforming Growth Factor-b1 in Small Airway Epithelium from Tobacco Smokers and Patients with Chronic Obstructive Pulmonary Disease (COPD)*. Am J Respir Crit Care Med. 2001 May; 163(6), 1476-1483

**[7]** Habashi, J. P., Judge, D. P., Holm, T. M., Cohn, R. D., Loeys, B. L., Cooper, T. K., … Dietz, H. C. (2006). *Losartan, an AT1 antagonist, prevents aortic aneurysm in a mouse model of Marfan syndrome*. Science (New York, N.Y.), 312(5770), 117–121.

**[8]** Neptune, R. Enid et al. *Dysregulation of TGF-β activation contributes to pathogensis in Marfan Syndrome*. Nature Genetics, 2003 Feb; 33, 408-411

**[9]** Kagami, S, Miller, D.E, Noble, N.A, *Angiotensin II stimulates extracellular matrix protein synthesis through induction of transforming growth factor-beta expression in rat glomerular mesangial cells.* J Clin Invest, 1994; 93(6):2431-2437

**[10]** Papp, M et al. *Angiotensin receptor subtype AT1 mediates alveolar epithelial cell apoptosis in response to ANG II.* Am J Physiol Lung Cell Mol Physiol 2002, 282: L713-L718

**[11]** Wong, M, H. Chapin, O, C. Johnson, M, D. *LPS-Stimulated Cytokine Production in Type I Cells Is Modulated by the Renin-Angiotensin System*. Am J Respir Cell Mol Bio, 2012, 46: 641-650

**[12]** Podowski, M, Wise, R, Neptune, E. *Angiotensin receptor blockade attenuates cigarette smoke-induced lung injury and rescues lung architecture in mic.* J Clin Invest. 2012;122(1):229-240

**[13]** Duncan, G, A. Jung, J. Hanes, J. Suk, J, S. *The Mucus Barrier to Inhaled Gene Therapy*. Mol Ther. 2016 Dec; 24(12): 2043-2053

**[14]** Donaldson, S, H. Corcoran, T, E. Laube, B, L. Bennett, W, D. *Mucociliary Clearance as an Outcome Measure for Cystic Fibrosis Clinical Research*. Proc Am Thorac Soc 2007 (4): 399-407

**[15]** Lai, S, K. Wang, Y, Y. Hanes, J. *Mucus-penetrating nanoparticles for drug and gene delivery to mucosal issues.* Adv Drug Deliv Rev. 2009 Feb; 61(2): 158-171

**[16]** Wang, Y, Y. Lai, S, K. Suk, J, S. Pace, A. Cone, R. Hanes, J. *Addressing the PEG Mucoadhesive Paradox to Engineer Nanoparticles that "Slip" through the Human Mucus Barrier.* Angew Chem Int Ed Engl. 2008; 47(50) 9726-9729

**[17]** Yu, T., Chisholm, J., Choi, W. J., Anonuevo, A., Pulicare, S., Zhong, W., … Hanes, J. *Mucus-Penetrating Nanosuspensions for Enhanced Delivery of Poorly Soluble Drugs to Mucosal Surfaces.* Advanced healthcare materials*,* 2016; *5*(21), 2745–2750

**[18]** Szapiel, S. et al. *Hereditary Emphysema in Tight-Skin (TsK/+) Mouse*. Am Rev Respir Dis 1981:123: 680-685

**[19]** Israili, ZH. *Clinical Pharmacokinetics of angiotensin II (AT1) receptor blockers in hypertension.* Journal of Human Hypertension. 2000; 14(1): S73-S86

**[20]** Yang, M., Lai, S. K., Wang, Y. Y., Zhong, W., Happe, C., Zhang, M., … Hanes, J. (2011). *Biodegradable nanoparticles composed entirely of safe materials that rapidly penetrate human mucus. Angewandte Chemie (International ed. in English)*, *50*(11), 2597–2600.

**[21]** Ensign, L, M. Tang, B,C. Wang, Y, Y. Tse, T, A. Hoen, T. Cone, R. Hanes, J. *Mucus-Penetrating Nanoparticles for Vaginal Drug Delivery Protect Against Herpes Simplex Virus*. Sci Transl Med. 2012 Jun; 4(138)

**[22]** Lee, J, H. Yeo, Y. *Controlled Drug Release from Pharmaceutical Nanocarriers.* Chem Eng Sci. 2015 Mar; 125: 75-84

**[23]** Zhou, J, L. Li, X, C. Garvin, J, L. Navar, L, G. Carretero, O, A. *Intracellular ANG II induces cytosolic Ca2+ mobilization by stimulating intracellular AT1 receptors in proximal tubule cells.* Am J Physiol Renal Phsiol. 2006 Jun; 290(6): F1382-F1390

**[24]** Das, S. MacDonald, K. Chag, H-Y, S. Mitzner, W. *A Simple Method of Mouse Lung Intubation*. Journal of Visualized Experiments. 2013 Mar: 7: e50318

**[25]** Zheng, T. Zhu, Z. Wang, Z. Ma, B. Elias, J. et al. *Inducible targeting of IL-13 to the adult lung causes matrix metalloproteinase- and cathepsin-dependent emphysema.*J Clin. Invest. 2000; 106: 1081-1093

**[26]** Lee, C, G. Zhu, Z. Lanon, S. Wan, X. Noble, P. Chen, Q, Elias, J. *Interleukin-13 Induces Tissue Fibrosis by Selectively Stimulating and Activating Transforming Growth Factor β1.* J Exp. Med. 2001 Sept; 194(6); 809-821

**[27]** Wrighton, K, H. Lin, X. Feng, X-H. *Phospho-control of TGF-β superfamily signaling.* Cell Res. 2009 Jan; 19(1): 8-20

**Curriculum Vitae**

# Michael G. Sweet

## EDUCATION

**MSE** Johns Hopkins University, Chemical and Biomolecular Engineering May 2019

Thesis: "Development of Angiotensin II Receptor Blocker Nanoparticles for an Inhaled Therapeutic Treatment of COPD via TGF-Beta Antagonism"

Advisor: Dr. Jung Soo Suk

**BS** Rensselaer Polytechnic Institute, Chemical Engineering May 2016

Minor in Economics

## RESEARCH EXPERIENCE

**Thesis, Johns Hopkins University**, Baltimore MD 2017 to 2019

Advisor: Dr. Jung Soo Suk

- Developed ARB nanocrystals for inhaled localize treatment
- Tested nanocrystal qualities on a COPD murine model
- Extensive work on particle separations and quantifications using HPLC

**Rensselaer Polytechnic Institute,** Troy NY 2016 to 2017

Advisor: Dr. Corey Woodcock, Dr. Joel Plawsky

- Aided in the development and testing of ultra-high heat flux heat sinks
- Co-author of paper published in the International Journal of Heat and Mass Transfer
  Woodcock, C. Ng'oma, C. **Sweet, M.** Wang, Y. Peles, Y. Joel, P.
  *Ultra-high heat flux dissipation with Piranha Pin Fins*
  Journal of Heat and Mass Transfer 2019 Jan; 128: 504-515